Hindawi
Complexity
Volume 2020, Article ID 7893451, 12 pages
https://doi.org/10.1155/2020/7893451

Research Article

Control of Near-Grazing Dynamics in the Two-Degree-of-Freedom Vibroimpact System with Symmetrical Constraints

Zihan Wang, Jieqiong Xu, Shuai Wu, and Quan Yuan

College of Mathematics and Information Science, Guangxi University, Nanning 530004, China

Correspondence should be addressed to Jieqiong Xu; xjq@gxu.edu.cn

Received 17 October 2019; Revised 16 February 2020; Accepted 2 March 2020; Published 10 April 2020

Guest Editor: Viet-Thanh Pham

The stability of grazing bifurcation is lost in three ways through the local analysis of the near-grazing dynamics using the classical concept of discontinuity mappings in the two-degree-of-freedom vibroimpact system with symmetrical constraints. For this instability problem, a control strategy for the stability of grazing bifurcation is presented by controlling the persistence of local attractors near the grazing trajectory in this vibroimpact system with symmetrical constraints. Discrete-in-time feedback controllers designed on two Poincare sections are employed to retain the existence of an attractor near the grazing trajectory. The implementation relies on the stability criterion under which a local attractor persists near a grazing trajectory. Based on the stability criterion, the control region of the two parameters is obtained and the control strategy for the persistence of near-grazing attractors is designed accordingly. Especially, the chaos near codimension-two grazing bifurcation points was controlled by the control strategy. In the end, the results of numerical simulation are used to verify the feasibility of the control method.

1. Introduction

Grazing bifurcation, one type of discontinuity-induced bifurcations, has been extensively studied in vibroimpact system as it has complex dynamics and is widely encountered in many engineering examples. On analysis of the dynamics near grazing in a general class of impact oscillator systems, a classical concept of analysis is the so-called discontinuity-mapping approach initially conceived of by Nordmark [1, 2] (see [3, 4] for an overview). The analysis is usually carried out by finding an appropriate local map describing the system dynamics in neighborhood of the grazing event. The local map can then be combined with an analytic Poincaré map to give the so-called grazing normal form whose dynamics can be shown to be topologically equivalent to those of the underlying flow. The grazing normal form derived by the discontinuity-mapping approach is used to analyze the local dynamics in the vicinity of a grazing trajectory. As shown in [5–8], the normal form map of the rigid impact oscillator contains a square-root term causing a singularity in the first derivative, which results in an abrupt loss of the stability. And different bifurcation scenarios associated with switching between impacting motions and nonimpacting motions near grazing were also described. In particular, the discontinuity-mapping approach was used by Fredriksson and Nordmark [9] to establish conditions for the persistence or disappearance of a local attractor in the vicinity of a grazing periodic trajectory. In addition, some conditions for the persistence of a local attractor in the immediate vicinity of quasiperiodic grazing trajectories in an impacting dynamical system were formulated by Thota and Dankowicz [10]. When the stability conditions of grazing bifurcation are degenerate, the codimension-two would occur, which is always a hot topic. Kowalczyk et al. [11] proposed a strategy for

classification of codimension-two discontinuity-induced bifurcations of limit cycles in piecewise smooth systems and studied their nonsmooth transitions. Foale [12] analyzed the results of a special codimension-two grazing bifurcation in a single-degree-of-freedom impact oscillator by using the impact surface as a Poincaré section. In addition, the study also shows that the bifurcation of the saddle node bifurcation and the flip bifurcation can meet at a certain codimension-two grazing points in the parameter plane. Thota et al. [13] studied the distribution of codimension-two grazing bifurcation point according to the discontinuous mapping in the single-degree-of-freedom collision oscillator and discussed the possible dynamic characteristics of the system response near this bifurcation point. Xu et al. [14] studied the codimension-two grazing bifurcation of n-degree-of-freedom vibrators with bilateral constraints and obtained and simplified the existence conditions of codimension-two grazing bifurcation. Similar phenomena about codimension-two grazing bifurcation can also be found in Refs. [15, 16]. Yin et al. [17] discussed the important role of some degenerated grazing bifurcation points in the transition between saddle node bifurcation and period doubling bifurcation. Dankowicz and Zhao [18, 19] studied the grazing bifurcations of the codimension-one and the codimension-two of a class of impact microactuators.

The loss of local attractors near grazing bifurcation may arise catastrophic changes of system response and lead to codimension-two or more complicated bifurcation; therefore, controlling near-grazing dynamics becomes necessary and significant. Dankowicz and Jerrelind [20] used the linear feedback control method to control the grazing bifurcation of the piece smooth dynamic system, so that the system has local attractors near the grazing orbit. Dankowicz and Svahn [21] presented for the existence of event-driven control strategies that guarantee the local persistence of system attractors with at most low-velocity contact in vibro impacting oscillators. Misra and Dankowicz [22] developed a rigorous control paradigm for regulating the near-grazing bifurcation behavior of limit cycles in piecewise-smooth dynamical systems. Yin et al. [23] analyzed the stability for near-grazing period-one impact motion to suppress grazing-induced instabilities. The bounded eigenvalues are further confined to the unit circle, and the continuous transition between the nonimpact motion and the controlled impact motion is obtained. Xu et al. [24] discussed the control problem of near-grazing dynamics in a two-degree-of-freedom vibroimpact system with a clearance.

Based on the concept of controlling the persistence of local attractors near the grazing trajectory in impact oscillator with unilateral constraints mentioned in [20–24], this paper aims to control the stability of grazing bifurcation or control the persistence of local attractors near the grazing trajectory in this vibroimpact system with symmetrical constraints. Compared with impact oscillator with unilateral constraint, the instability problems near grazing trajectory become more complex for impact oscillator with symmetrical constraints as mentioned in [17]. The stability of double grazing motion bifurcation in the system is lost in three ways, and the existence conditions of the codimension-two grazing bifurcation occur in four different cases accordingly. For this complex unstable problem, analytic expressions of stability criterion are obtained in this paper. Based on the stability criterion, the stability control strategy of the persistence of near-grazing attractors is proposed. Furthermore, the chaos near codimension-two grazing bifurcation points was controlled by the control strategy. This paper is organized as follows. In Section 2, a two-degree-of-freedom vibroimpact system with symmetrical constraints is introduced. In Section 3, near-grazing bifurcation dynamics are analyzed. In Section 4, the discrete-in-time feedback control method is designed to maintain the persistence of the local attractor of double grazing period motion. In Section 5, numerical simulation is used to verify the feasibility of the control method. Finally, the conclusion is given in Section 6.

2. Mechanical Model and Double Grazing Periodic Motion

Figure 1 shows the schematic model of a two-degree-of-freedom impact oscillator with a clearance. Masses M_1 and M_2 are connected to linear viscous dampers C_1 and C_2 by linear springs with stiffness K_1 and K_2, respectively. The harmonic forces of the amplitude P_1 and P_2 are applied to the masses M_1 and M_2, respectively, and the harmonic force is applied only to the mass in the horizontal direction. The mass M_1 moves between the symmetrical rigid stops A and C. When the mass M_1 strikes rigid stop A or C, the motion becomes a nonlinear motion and the impact is described by the recovery factor R. Assuming that the damping in the mechanical model is the Rayleigh type proportional damping, it can be known that $(C_1/K_1) = (C_2/K_2)$.

The governing equation is described by

$$\begin{bmatrix} M_1 & 0 \\ 0 & M_2 \end{bmatrix}\begin{bmatrix} \ddot{X}_1 \\ \ddot{X}_2 \end{bmatrix} + \begin{bmatrix} C_1 & -C_1 \\ -C_1 & C_1 + C_2 \end{bmatrix}\begin{bmatrix} \dot{X}_1 \\ \dot{X}_2 \end{bmatrix} + \begin{bmatrix} K_1 & -K_1 \\ -K_1 & K_1 + K_2 \end{bmatrix}\begin{bmatrix} X_1 \\ X_2 \end{bmatrix} = \begin{bmatrix} P_1 \\ P_2 \end{bmatrix}\sin(\Omega T + \tau), \quad \left(|X_1| < D\right). \tag{1}$$

When $|X_1| = D$, the collision occurs. At this time, the collision equation is as follows:

$$\dot{X}_{1+} = -R\dot{X}_{1-}, \quad \left(|X_1| = D\right), \tag{2}$$

where $\dot{X}$ and $\ddot{X}$ represent the first and second derivatives of X with respect to time T, respectively. $\dot{X}_{1+}$ indicates the instantaneous speed at which the mass M_1 approaches the

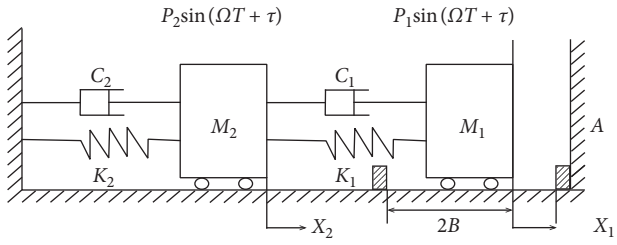

Figure 1: Schematic of the two-degree-of-freedom impact oscillator with symmetrical constraints.

rigid stop A or C. $\dot{X}_{1-}$ indicates the instantaneous speed at which the mass M_1 leaves the rigid stop A or C.

Introduce the nondimensional quantities as follows:

$$\begin{aligned}
\mu_m &= \frac{M_2}{M_1},\\
\mu_k &= \frac{K_2}{K_1},\\
\mu_c &= \frac{C_2}{C_1},\\
\mu_c &= \mu_k,\\
p &= \frac{P_2}{P_1+P_2},\\
\omega &= \Omega\sqrt{\frac{M_1}{K_1}},\\
t &= T\sqrt{\frac{K_1}{M_1}},\\
\zeta &= \frac{C_1}{2\sqrt{K_1M_1}},\\
d &= \frac{DK_1}{P_1+P_2},\\
x_1 &= \frac{X_1K_1}{P_1+P_2},\\
x_2 &= \frac{X_2K_1}{P_1+P_2}.
\end{aligned} \tag{3}$$

According to equations (1)–(3), the system can be transformed into nondimensional forms.

$$\begin{bmatrix} 1 & 0\\ 0 & \mu_m \end{bmatrix}\begin{bmatrix} \ddot{x}_1\\ \ddot{x}_2 \end{bmatrix} + \begin{bmatrix} 2\zeta & -2\zeta\\ -2\zeta & 2\zeta(1+\mu_c) \end{bmatrix}\begin{bmatrix} \dot{x}_1\\ \dot{x}_2 \end{bmatrix} + \begin{bmatrix} 1 & -1\\ -1 & 1+\mu_k \end{bmatrix}\begin{bmatrix} x_1\\ x_2 \end{bmatrix} = \begin{bmatrix} 1-p\\ p \end{bmatrix}\sin(\omega t+\tau), \quad \left(|x_1|<d\right), \tag{4}$$

$$\dot{x}_{1+} = -R\dot{x}_{1-}, \quad \left(|x_1| = d\right), \tag{5}$$

where $\dot{x}$ and $\ddot{x}$ represent the first and second derivatives of x with respect to the nondimensional time t, respectively.

Suppose Ψ be the canonical modal matrix of equation (4), and coordinate transformation of equation (4). Let $x = \Psi\xi$ 4.

(4)

$$I\ddot{\xi} + C\dot{\xi} + \Lambda\xi = P\sin(\omega t+\tau), \tag{6}$$

where ω_1 and ω_2 represent the eigenfrequencies of the system, $x = (x_1, x_2)^T$, $\xi = (\xi_1, \xi_2)^T$, I is the unit matrix, Λ and C are diagonal matrices, $\Lambda = \mathrm{diag}[\omega_1^2, \omega_2^2]$, $C = 2\zeta\Lambda = \mathrm{diag}[2\zeta\omega_1^2, 2\zeta\omega_2^2]$, and $P = \Psi^T(1-p, p)^T$. The general solution of equation (4) is given by

$$\begin{aligned}
x_i &= \sum_{j=1}^{2}\Psi_{ij}\Big(e^{-\eta_j(t-t_0)}\left(a_j\cos\omega_{dj}t + b_j\cos\omega_{dj}t\right)\\
&\quad + A_j\sin(\omega t+\tau) + B_j\cos(\omega t+\tau)\Big),\\
\dot{x}_i &= \sum_{j=1}^{2}\Psi_{ij}\Big(e^{-\eta_j(t-t_0)}\Big(\left(b_j\omega_{dj} - a_j\eta_j\right)\cos\omega_{dj}t\\
&\quad -\left(a_j\omega_{dj} + b_j\eta_j\right)\sin\omega_{dj}t\Big)\\
&\quad + A_j\omega\cos(\omega t+\tau) - B_j\omega\sin(\omega t+\tau)\Big),
\end{aligned} \tag{7}$$

where $i = 1, 2$, t_0 represents the time at which the mass M_1 collides with the rigid stop A or C; we set the mass M_1 to collide with the rigid stop A when $t_0 = 0$. Ψ_{ij} is an element of the canonical modal matrix Ψ, $\eta_j = \zeta\omega_j^2$, and $\omega_{dj} = \sqrt{\omega_j^2 - \eta_j^2}$. The initial conditions and modal parameters of the system determine the integral constants a_j and b_j. A_j and B_j are amplitude parameters, and the expression is given by

$$\begin{aligned}
A_j &= \frac{1}{2\omega_{dj}}\left(\frac{\omega+\omega_{dj}}{\left(\omega+\omega_{dj}\right)^2+\eta_j^2} - \frac{\omega-\omega_{dj}}{\left(\omega-\omega_{dj}\right)^2+\eta_j^2}\right)\overline{f}_j,\\
B_j &= \frac{\eta_j}{2\omega_{dj}}\left(\frac{1}{\left(\omega+\omega_{dj}\right)^2+\eta_j^2} - \frac{1}{\left(\omega-\omega_{dj}\right)^2+\eta_j^2}\right)\overline{f}_j.
\end{aligned} \tag{8}$$

According to the initial conditions and periodic conditions of the double grazing periodic-n motion, the existence conditions of two-degree-of-freedom impact oscillator double grazing periodic-n motion is as follows:

$$d = \sqrt{d_1^2 + d_2^2},$$
$$\tau = \arctan\left(\frac{d_1}{d_2}\right), \tag{9}$$

where $d_1 = \Psi_{11}A_1 + \Psi_{12}A_2$ and $d_2 = \Psi_{11}B_1 + \Psi_{12}B_2$.

In addition, in order to ensure that the impacting cycle of the mass M_1 does not adhere to rigid stop, the acceleration a^* of the mass M_1 satisfies $a^* < 0$ and the acceleration a^* of the mass M_2 satisfies $a^* > 0$.

3. Near-Grazing Dynamics

3.1. The Stability Criterion of Double Grazing Bifurcation. Let p be a state vector, such that $x = (x_1, v_1, x_2, v_2, p)^T \in R^5$, and it follows that

$$\frac{\mathrm{d}x}{\mathrm{d}t} = \dot{x} = f(x) = (v_1, a_1, v_2, a_2, 0)^T, \tag{10}$$

where a_i represents the acceleration of the oscillator as a function of x_i, v_i. Define $\phi(x,t)$ as the local flow function associated with $f(x)$. Suppose that the movement of the oscillator is limited by symmetrical rigid constraints placed at $|x_1| = d$ corresponding to state space discontinuity surfaces D_1 and D_2, where

$$D_1 = h^{D_1}(x,d) = d - x_1 = 0,$$
$$D_2 = h^{D_2}(x,d) = -d - x_1 = 0. \tag{11}$$

The oscillator moves between two rigid stops when $h^{D_1}(x,d) > 0$ and $h^{D_2}(x,d) < 0$. When $h^{D_1}(x,d) = 0$ or $h^{D_2}(x,d) = 0$, the oscillator collides with the rigid stop. In addition, let $h^{P_1}(x) = h_x^{D_1}(x,d)f(x) = -v_1$, $h_x^{P_2}(x) = h^{D_2}(x,d)f(x) = -v_1$.

When the oscillator collides with the constraint, we establish a function $R(x)$ with a characteristic restitution coefficient R to represent the jump map, i.e., $R(x)$ represents the instantaneous state after the collision and before the collision, where

$$R(x) = (x_1, -Rv_1, x_2, v_2, p)^T. \tag{12}$$

The state space trajectory and the grazing contact points of D_1 and D_2 are, respectively, corresponding to points x^{*1} and x^{*2}, so that

$$\begin{aligned}
&h^{D_1}(x^{*1}, d^*) = 0,\\
&h^{P_1}(x^{*1}) = -v_1^{*1} = 0,\\
&\frac{\mathrm{d}}{\mathrm{d}t}h^{P_1}(x)\Big|_{x=x^{*1}} = h_x^{P_1}(x^{*1})f(x^{*1}) = -a_1^{*1} > 0,\\
&h^{D_2}(x^{*2}, d^*) = 0,\\
&h^{P_2}(x^{*2}) = -v_1^{*2} = 0,\\
&\frac{\mathrm{d}}{\mathrm{d}t}h^{P_2}(x)\Big|_{x=x^{*2}} = h_x^{P_2}(x^{*2})f(x^{*2}) = -a_1^{*2} < 0.
\end{aligned} \tag{13}$$

Choose a constant phase angle θ^* as a Poincaré section, and it has the following form: $\Pi_1 = \{\hat{x} \in R^5 \times S^1 \mid \theta = \theta^*\}$, where $\hat{x} = (x_1, \dot{x}_1, x_2, \dot{x}_2, p, \theta)^T$, $\theta = \omega t + \tau$. The modulus of θ is 2π, $\theta^* = \tau^*$. Since the periodic trajectory of the system is symmetrical, we set another Poincaré section as $\Pi_2 = \{\hat{x} \in R^5 \times S^1 \mid \theta = \theta^* + \pi\}$.

With d as the bifurcation parameter, we define the flow maps $P_1(x)$ and $P_2(x)$ by the evolution of the smooth flow $\Phi(\cdot, T)$ on the Poincaré sections Π_1 and Π_2; the expressions of $P_1(x)$ and $P_2(x)$ are as follows:

$$P_1(x) = x^{*2} + N_1\left(x - x^{*1}\right) + M_1\left(d - d^*\right) + \text{h.o.t}, \tag{14}$$

where $N_1 = (\partial/\partial x)P_1(x)|_{x=x^{*1},d=d^*}$ and $M_1 = (\partial/\partial d)P_1(x)|_{x=x^{*1},d=d^*}$.

$$P_2(x) = x^{*1} + N_2\left(x - x^{*2}\right) + M_2\left(d - d^*\right) + \text{h.o.t}, \tag{15}$$

where $N_2 = (\partial/\partial x)P_2(x)|_{x=x^{*2},d=d^*}$ and $M_2 = (\partial/\partial d)P_2(x)|_{x=x^{*2},d=d^*}$.

The critical bifurcation value d^* can be obtained from expression (9). Since the vector field $f(x)$ and the smooth flow function $\Phi(\cdot, T)$ do not contain the bifurcation parameter d, the values of the matrices $M_1 = M_2 = 0$.

We use the discontinuous mapping method introduced by Nordmark to analyze the system; the two discontinuous maps DM_1 and DM_2 are introduced into the neighborhood of points x^{*1} and x^{*2} such that the surface $P_1(x)$ is invariant under DM_1,i.e., $x \in P_1(x)$, $DM_1(x) \in P_1(x)$. The same surface $P_2(x)$ is invariant under DM_2, i.e., $x \in P_2(x)$, $DM_2(x) \in P_2(x)$. According to the discontinuous mapping method, the discontinuous mapping of DM_1 and DM_2 is expressed by

$$DM_1 = \begin{cases} Id, & h^{D_1}(x,d) \geq 0,\\ x^{*1} + \beta_1\sqrt{\dfrac{2}{h_x^{P_1}(x^{*1})f(^{*1})}}\sqrt{-h^{D_1}(x,d)}, & h^{D_1}(x,d) < 0, \end{cases} \tag{16}$$

where

$$\beta_1 = f\left(x^{*1}\right) - g_x\left(x^{*1}\right)f\left(x^{*1}\right),$$

$$DM_2 = \begin{cases} Id, & h^{D_2}(x,d) \leq 0,\\ x^{*2} + \beta_2\sqrt{\dfrac{2}{h_x^{P_2}(x^{*2})f(^{*2})}}\sqrt{-h^{D_2}(x,d)}, & h^{D_2}(x,d) > 0, \end{cases} \tag{17}$$

where

$$\beta_2 = f\left(x^{*2}\right) - g_x\left(x^{*2}\right)f\left(x^{*2}\right). \tag{18}$$

According to (13)–(17), the composite maps $\tilde{P}_1 = P_1(x) \circ DM_1$ and $\tilde{P}_2 = P_2(x) \circ DM_2$ are written as

$$\widetilde{P}_1 = \begin{cases} x^{*2} + N_1\left(x - x^{*1}\right) + \text{h.o.t}, & h^{D_1}(x,d) \geq 0, \\ x^{*2} + N_1\beta_1\sqrt{\dfrac{2}{h_x^{P_1}(x^{*1})f(x^{*1})}}\sqrt{-h^{D_1}(x,d)} + \text{h.o.t}, & h^{D_1}(x,d) < 0, \end{cases} \tag{19}$$

$$\widetilde{P}_2 = \begin{cases} x^{*1} + N_2\left(x - x^{*2}\right) + \text{h.o.t}, & h^{D_2}(x,d) \leq 0, \\ x^{*1} + N_2\beta_2\sqrt{\dfrac{2}{h_x^{P_2}(x^{*2})f(x^{*2})}}\sqrt{-h^{D_2}(x,d)} + \text{h.o.t}, & h^{D_2}(x,d) > 0. \end{cases} \tag{20}$$

We will discuss the stability of double grazing bifurcation using the Poincaré map $\widetilde{P} = \widetilde{P}_2 \circ \widetilde{P}_1$. Starting from the vicinity of the grazing point, whether it is at the impact side or the nonimpact side, if it is still close to the grazing point after the iterative mapping $\widetilde{P}$, then the local attractor near the grazing trajectory exists; we refer to such scenario as a continuous grazing bifurcation or we say that the grazing bifurcation is stable. Otherwise, we refer to scenario as a discontinuous grazing bifurcation.

When point x starts from the impact side near the grazing point x^{*1}, $h^{D_1}(x,d) < 0$. Here, we can think of the $h^{D_1}(x,d)$ approximation as $h_x^{D_1}(x^{*1})(x - x^{*1})$. Similarly, we consider the $h^{D_2}(x,d)$ approximation as $h_x^{D_2}(x^{*2})(x - x^{*2})$.

If

$$h_x^{D_2}\left(x^{*2}\right)\left(\widetilde{P}_1(x) - x^{*2}\right) = h_x^{D_2}\left(x^{*2}\right)N_1\beta_1\sqrt{\frac{2}{h_x^{P_1}(x^{*1})f(x^{*1})}}\sqrt{-h^{D_1}(x,d)} \leq 0, \tag{21}$$

it means $\widetilde{P}_1(x)$ is located at the nonimpact side near the grazing point x^{*2}.

After the iteration of the mapping $\widetilde{P}_2$, if

$$h_x^{D_1}\left(x^{*1}\right)\left(\widetilde{P}_2\widetilde{P}_1(x) - x^{*1}\right) = h_x^{D_1}\left(x^{*1}\right)N_2N_1\beta_1\sqrt{\frac{2}{h_x^{P_1}(x^{*1})f(x^{*1})}}\sqrt{-h^{D_1}(x,d)} < 0, \tag{22}$$

then,

$$h_x^{D_1}\left(x^{*1}\right)N_2N_1\beta_1 < 0. \tag{23}$$

It means the impact point impacts discontinuity surface D_1 again and the impact will be perpetuated, which results in a large stretching in a direction given by the image of the vector β_1 under the Jacobian N_1 and N_2. Therefore, the local attractor near the grazing trajectory does not exist. According to the analysis, the stability criterion of grazing bifurcation under which a local attractor persists near a grazing trajectory is formulated as follows:

$$h_x^{D_2}\left(x^{*2}\right)N_1\left(N_2N_1\right)^{(n-1)}\beta_1 \leq 0, \tag{24}$$

and

$$h_x^{D_1}\left(x^{*1}\right)\left(N_2N_1\right)^n\beta_1 \geq 0, \tag{25}$$

for all positive integer n.

According the same method, another stability criterion of grazing bifurcation under which a local attractor persists near a grazing trajectory is formulated as follows:

$$h_x^{D_1}\left(x^{*1}\right)N_2\left(N_1N_2\right)^{(n-1)}\beta_2 \geq 0, \tag{26}$$

and

$$h_x^{D_2}\left(x^{*2}\right)\left(N_1N_2\right)^n\beta_2 \leq 0, \tag{27}$$

for all positive integer n.

3.2. Codimension-Two Grazing Bifurcation. The local attractor near grazing trajectory is lost in there ways.

Case 1. If

$$h^{D_2}\left(x^{*2}\right)\left(\widetilde{P}_1(x), d\right) = h_x^{D_2}\left(x^{*2}\right)N_1\beta_1\sqrt{\frac{2}{h_x^{P_1}(x^{*1})f(x^{*1})}}\sqrt{-h^{D_1}(x,d)} < 0, \tag{28}$$

i.e., $h_x^{D_2}(x^{*2})N_1\beta_1 < 0$, and

$$h^{D_1}\left(x^{*1}\right)\left(\widetilde{P}_2\left(\widetilde{P}_1(x)\right), d\right) = h_x^{D_1}\left(x^{*1}\right)N_2N_1\beta_1\sqrt{\frac{2}{h_x^{P_1}(x^{*1})f(x^{*1})}}\sqrt{-h^{D_1}(x,d)} < 0, \tag{29}$$

i.e., $h_x^{D_1}(x^{*1})N_2N_1\beta_1 < 0$, then it means that the point from the impact side near the grazing point x^{*1} will impact the discontinuous surface D_1 again after the iteration of the mapping $\widetilde{P}$ and the impact will continue, which results in a large stretching in a direction given by the image of the vector β_1 under the Jacobian N_1 and N_2; therefore, the local near-grazing attractor will lose, where discontinuous grazing bifurcation occurs.

If the impact point is followed by nonimpacting for some iterations but eventually impacts discontinuous surface D_1, the impact will be perpetuated which lead to the instability of grazing bifurcation or the loss of near-grazing attrators.

Therefore,

$$h_x^{D_2}\left(x^{*2}\right)N_1\left(N_2N_1\right)^i\beta_1<0,$$
$$h_x^{D_1}\left(x^{*1}\right)\left(N_2N_1\right)^{j+1}\beta_1<0, \tag{30}$$

for any $0\le i\le j$, the stability of grazing bifurcation will be lost, where i and j are positive integers.

Case 2. When the point x satisfying $h_x^{D_1}(x-x^{*1})<0$ is from the impact side near the grazing point x^{*1}, if $h_x^{D_2}(x^{*2})N_1\beta_1>0$ and $h_x^{D_2}(x^{*2})N_1N_2\beta_2>0$, it means that the impact point will impact with the discontinuous surface D_2 again and the impact will continue, and the grazing bifurcation is discontinuous.

If the impact point is followed by nonimpacting for some iterations but eventually impacts discontinuous surface D_2, the impact will be perpetuated. Finally, the stability of grazing bifurcation will also be lost.

That is,

$$h_x^{D_2}\left(x^{*2}\right)N_1\left(N_2N_1\right)^i\beta_1>0,$$
$$h_x^{D_2}\left(x^{*2}\right)\left(N_1N_2\right)^{j+1}\beta_2>0, \tag{31}$$

for any $j\ge i\ge 0$, the stability of grazing bifurcation will be lost.

Case 3. When the point x satisfying $h_x^{D_1}(x-x^{*1})<0$ is from the impact side near the grazing point x^{*1}, if $h_x^{D_2}(x^{*2})N_1\beta_1>0$ and $h_x^{D_1}(x^{*1})N_2\beta_2<0$, this means that the impact point will impact with the discontinuous surfaces D_1 and D_2 again and the impact will continue, and the grazing bifurcation is discontinuous. If the impact point is followed by non-impacting for some iterations but eventually impacts discontinuous surface D_1 and D_2 the impact will be perpetuated. Finally, the stability of grazing bifurcation will also be lost.

That is,

$$h_x^{D_2}\left(x^{*2}\right)N_1\left(N_2N_1\right)^i\beta_1>0,$$
$$h_x^{D_1}\left(x^{*1}\right)N_2\left(N_1N_2\right)^j\beta_2<0, \tag{32}$$

for any $j\ge i\ge 0$, the stability of grazing bifurcation will be lost.

According to the above analysis, the conditions of codimension-two grazing bifurcation are obtained as follows (the definition of such points is seen in Ref. [10]):

$$h_x^{D_1}\left(x^{*1}\right)\left(N_2N_1\right)^n\beta_1=0,$$
$$h_x^{D_1}\left(x^{*1}\right)N_2\left(N_1N_2\right)^n\beta_2=0,$$
$$h_x^{D_2}\left(x^{*2}\right)N_1\left(N_2N_1\right)^n\beta_1=0,$$
$$h_x^{D_2}\left(x^{*2}\right)\left(N_1N_2\right)^n\beta_2=0, \tag{33}$$

where $n=0,1,2,\ldots$.

4. Controlling the Persistence of Near-Grazing Attractors

As the lose of stability for grazing bifurcation may arise catastrophic changes of system response and codimension-two even more complicated bifurcation, it is necessary to control the stability of grazing bifurcation by controlling the persistence of the local near-grazing attractor. We use discrete-in-time feedback control to stabilize the grazing bifurcation. Two constant phase angles are defined as Poincaré sections, and two discrete-in-time feedback controllers on Poincaré sections are designed. After that, we obtain a new compound map and then control the stability of the grazing bifurcation by controlling the parameters on the controller.

We define the other two constant phase angles as Poincaré sections Π_3 and Π_4, where $\Pi_3=\{\widehat{x}\in R^5\times S^1\mid\theta=\theta^*+(\pi/2)\}$ and $\Pi_4\{\widehat{x}\in R^5\times S^1\mid\theta=\theta^*+(3\pi/2)\}$.

According to $P_1(x)$ and Π_3, we define the mappings $P_3(x)$: $\Pi_1\longrightarrow\Pi_3$ and $P_4(x)$: $\Pi_3\longrightarrow\Pi_2$, and the resulting expansion is as follows:

$$P_3(x)=x^{*3}+N_3\left(x-x^{*1}\right)+\text{h.o.t},$$
$$P_4(x)=x^{*2}+N_4\left(x-x^{*3}\right)+\text{h.o.t}, \tag{34}$$

where x^{*3} is the fixed point of the grazing orbit on the Poincaré section Π_3, $N_3=(\partial/\partial x)P_3(x)|_{x=x^{*1}}$, and $N_4=(\partial/\partial x)P_4(x)|_{x=x^{*3}}$.

In the same way, according to $P_2(x)$ and Π_4, we define the mappings $P_5(x)$: $\Pi_2\longrightarrow\Pi_4$ and $P_6(x)$: $\Pi_4\longrightarrow\Pi_1$, and the expansion is as follows:

$$P_5(x)=x^{*4}+N_5\left(x-x^{*2}\right)+\text{h.o.t},$$
$$P_6(x)=x^{*1}+N_6\left(x-x^{*4}\right)+\text{h.o.t}, \tag{35}$$

where x^{*4} is the fixed point of the grazing orbit on the Poincaré section Π_4, $N_5=(\partial/\partial x)P_5(x)|_{x=x^{*2}}$, and $N_6=(\partial/\partial x)P_6(x)|_{x=x^{*4}}$.

Discrete-in-time feedback controllers are designed on the Poincaré sections Π_3 and Π_4, respectively, as follows:

$$G_1(x)=\begin{bmatrix}x_1\\ v_1\\ x_2\\ v_2\\ k_1\left(x_1-x_1^{*3}\right)+k_2\left(v_1-v_1^{*3}\right)+k_3\left(p-p^*\right)+p^*\end{bmatrix},$$
$$G_2(x)=\begin{bmatrix}x_1\\ v_1\\ x_2\\ v_2\\ k_4\left(x_1-x_1^{*4}\right)+k_5\left(v_1-v_1^{*4}\right)+k_6\left(p-p^*\right)+p^*\end{bmatrix}. \tag{36}$$

We can calculate the expressions of maps $G_1(x)$ and $G_2(x)$ which have the following forms:

$$\begin{aligned} G_1(x) &= x_1^{*3} + G_{1x}\left(x - x_1^{*3}\right), \\ G_2(x) &= x_1^{*4} + G_{2x}\left(x - x_1^{*4}\right), \end{aligned} \tag{37}$$

where

$$\begin{aligned} G_{1x} &= \begin{bmatrix} 1 & 0 & 0 & 0 & 0 \\ 0 & 1 & 0 & 0 & 0 \\ 0 & 0 & 1 & 0 & 0 \\ 1 & 0 & 0 & 1 & 0 \\ k_1 & k_2 & 0 & 0 & k_3 \end{bmatrix}, \\ G_{2x} &= \begin{bmatrix} 1 & 0 & 0 & 0 & 0 \\ 0 & 1 & 0 & 0 & 0 \\ 0 & 0 & 1 & 0 & 0 \\ 1 & 0 & 0 & 1 & 0 \\ k_4 & k_5 & 0 & 0 & k_6 \end{bmatrix}. \end{aligned} \tag{38}$$

The combining the map $G_1(x)$ and $P_3(x)$, $P_4(x)$, obtain a controlled map as $P_{g1}(x) = P_4(x) \circ G_1(x) \circ P_3(x)$, expansion as follows:

$$P_{g1}(x) = x^{*2} + N_4 G_{1x} N_3\left(x - x^{*1}\right) + \text{h.o.t}, \tag{39}$$

where $G_{1x} = (\partial/\partial x) G_1(x)|_{x=x^{*3}}$.

Similarly, combining the map $G_2(x)$ with the map $P_5(x)$, $P_6(x)$, the map under control $P_{g2}(x) = P_6(x) \circ G_2(x) \circ P_5(x)$, is obtained and its expansion has the following forms:

$$P_{g2}(x) = x^{*1} + N_6 G_{2x} N_5\left(x - x^{*2}\right) + \text{h.o.t}, \tag{40}$$

where $G_{2x} = (\partial/\partial x) G_2(x)|_{x=x^{*4}}$.

We can calculate the expressions of N_i as follows:

$$N_i = \begin{bmatrix} \triangle & \triangle & \triangle & \triangle & \triangle \\ \triangle & \triangle & \triangle & \triangle & \triangle \\ \triangle & \triangle & \triangle & \triangle & \triangle \\ \triangle & \triangle & \triangle & \triangle & \triangle \\ 0 & 0 & 0 & 0 & 1 \end{bmatrix}, \tag{41}$$

where $i = 3, 4, 5, 6$ and the symbol Δ refers to a nontrivial coefficient.

Combining (39) and (15), we construct a composite map of $\widetilde{P}_{g1} = P_{g1}(x) \circ DM_1$; the expressions are as follows:

$$\widetilde{P}_{g1} = \begin{cases} x^{*2} + N_{g1}\left(x - x^{*1}\right) + \text{h.o.t}, & h^{D_1}(x, d) \geq 0, \\ x^{*2} + N_{g1}\beta_1 \sqrt{\dfrac{2}{h_x^{P_1}(x^{*1}) f(x^{*1})}} \sqrt{-h^{D_1}(x, d)} + \text{h.o.t}, & h^{D_1}(x, d) < 0, \end{cases} \tag{42}$$

where $N_{g1} = N_4 G_{1x} N_3$.

Similarly, we can combine (40) and (17) to construct a composite map of $\widetilde{P}_{g2} = P_{g2}(x) \circ DM_2$; the expression is as follows:

$$\widetilde{P}_{g2} = \begin{cases} x^{*1} + N_{g2}\left(x - x^{*2}\right)\text{h.o.t}, & h^{D_2}(x, d) \leq 0, \\ x^{*1} + N_{g2}\beta_2 \sqrt{\dfrac{2}{h_x^{P_2}(x^{*2}) f(x^{*2})}} \sqrt{-h^{D_2}(x, d)} + \text{h.o.t}, & h^{D_2}(x, d) > 0, \end{cases} \tag{43}$$

where $N_{g2} = N_6 G_{2x} N_2$.

According to the analysis in Section 3, there are three cases in which the grazing bifurcation is unstable, where discontinuous grazing bifurcation occurs. For Case 1, the impact point will impact with the discontinuous surface D_1 again after some iterations and the impact will be perpetuated. Based on the stability criteria (24) and (25), we control $k_1 - k_6$ on the controller to ensure that $h_x^{D_2}(x^{*2}) N_{g1} (N_{g2} N_{g1})^{n-1} \beta_1 \leq 0$ and $h_x^{D_1}(x^{*1}) (N_{g2} N_{g1})^n \beta_1 \geq 0$, for positive integer n, such that the grazing bifurcation will be continuous.

For Case 2, the impact point will impact with the discontinuous surface D_2 again after some iterations and the impact will be perpetuated. Based on the stability criteria (26) and (27), we control $k_1 - k_6$ on the controller so that $h_x^{D_2}(x^{*2}) (N_{g1} N_{g2})^n \beta_2 \leq 0$ and $h_x^{D_1}(x^{*1}) N_{g2} (N_{g1} N_{g2})^{n-1} \beta_2 \geq 0$ for positive integer n. The grazing bifurcation will be continuous.

For Case 3, the impact point will impact with the discontinuous surfaces D_1 and D_2 again, and after some iterations, the impact will be perpetuated. Based on the stability criteria (24) and (25) or (26) and (27), the grazing bifurcation will be continuous by controlling parameters $k_1 - k_6$ to ensure the local attractor near grazing bifurcation persists.

For the codimension-two grazing bifurcation point, the persistence of near-grazing attractors is also controlled by controlling $k_1 - k_6$ based on the stability criteria (24) and (25) or (26) and (27). For example, if $h_x^{D_1}(x^{*1})(N_2 N_1)^n \beta_1 = 0$, we might let $h_x^{D_2}(x^{*2}) N_{g1} (N_{g2} N_{g1})^{n-1} \beta_1 \le 0$ and $h_x^{D_1}(x^{*1})(N_{g2} N_{g1})^n \beta_1 \ge 0$ by controlling $k_1 - k_6$.

If $h_x^{D_1}(x^{*1}) N_2 (N_1 N_2)^n \beta_2 = 0$, we might let $h_x^{D_2}(x^{*2})(N_{g1} N_{g2})^n \beta_2 \le 0$ and $h_x^{D_1}(x^{*1}) N_{g2} (N_{g1} N_{g2})^{n-1} \beta_2 \ge 0$ by controlling $k_1 - k_6$.

5. Numerical Experiments

For this system, we take suitable parameters $\mu_m = 6.0$, $\mu_k = 3.0$, $\omega = 0.63$, $R = 0.82$, $\zeta = 0.2$, and $p = 2.513$ as an example. d is supposed as the bifurcation parameter; the critical value $d^* = 1.61139$ for grazing bifurcation is obtained from formula (9). According to the analysis of near-grazing dynamics in Section 3, under the set of fixed parameters, $h_x^{D_2}(x^{*2}) N_1 \beta_1 = -0.128027 < 0$ and $h_x^{D_1}(x^{*1}) N_2 N_1 \beta_1 = -0.078865 < 0$. The impact point will impact with the discontinuous surfaces D_1 again and the impact will be perpetuated, which satisfies the instability conditions in Case 1. The bifurcation diagram as shown in Figure 2(a) is obtained through numerical simulation by discontinuity maps (19) and (20). It is clear that the grazing bifurcation is discontinuous because the discontinuous transition occurs at the bifurcation point $d - d^* = 0$. In addition, we take Π_2 as the Poincaré section; the bifurcation diagram as shown in Figure 2(b) is obtained through direct numerical simulation by (4) and (5), and it is clear that the discontinuous jump also occurs at the grazing bifurcation point $d - d^* = 0$.

We use the control method in Section 4 to stabilize the unstable grazing bifurcation phenomena. When the parameters of k_1, k_3 and $k_4, k_6$are fixed, the ranges of parameters k_2 and k_5 are calculated according to control strategy, which is named two-dimensional control region of k_2 and k_5. Here, we select $k_1 = -0.5$, $k_3 = -1$, $k_4 = -0.5$, and $k_6 = -1$ as the fixed parameters; a two-dimensional control region graph of k_2 and k_5 is obtained as shown in Figure 3(a), where k_2 is $x-$axis, k_5 is $y-$axis, and the blue region is the region of control parameters for ensuring the stability of the grazing bifurcation.

We select $k_2 = -5.8$ and $k_5 = -5.8$ to control the system and draw Figure 4(a) through the discontinuity maps (40) and (41). At the same time, we take Π_2 as the Poincaré section and obtain Figure 4(b) by direct numerical simulation. As shown in Figures 4(a) and 4(b), there exists the local attractor near grazing bifurcation.

Take the set of parameters $\mu_m = 6.0$, $\mu_k = 3.0$, $\omega = 0.48$, $R = 0.82$, $\zeta = 0.2$, $p = 2.013$, as an example. $d^* = 0.65183$, is obtained from equation (9). Without control, $h_x^{D_2}(x^{*2}) N_1 N_2 N_1 \beta_1 = -0.00868998 < 0$ and $h_x^{D_1}(x^{*1})(N_2 N_1)^2 \beta_1 = -0.00822255 < 0$. are obtained under the above fixed parameters. It satisfies the instability conditions in case 1 according to expression (30). The bifurcation diagram as shown in Figure 2(c) is obtained through numerical simulation by discontinuity maps (19) and (20). It is clear that the grazing bifurcation is discontinuous because the discontinuous transition occurs at the bifurcation point $d - d^* = 0$. In addition, we take Π_2 as the Poincaré section, and the bifurcation diagram as shown in Figure 2(d) is obtained through direct numerical simulation by (4) and (5); it is clear that the discontinuous jump also occurs at the grazing bifurcation point $d - d^* = 0$.

Based on the stability criterion mentioned in Section 4, we select $k_1 = -0.6$, $k_3 = -1$, $k_4 = -0.6$, and $k_6 = -1$ as the fixed parameters; a two-dimensional control region graph of k_2 and k_5 is obtained as shown in Figure 3(b), where k_2 is $x-$axis, k_5 is $y-$axis, and the blue region is the region of control parameters for ensuring the stability of the grazing bifurcation. Then, we select $k_2 = -5.8$ and $k_5 = -5.8$ to control the system, and the bifurcation diagram is obtained as shown in Figure 4(c) by the discontinuity maps (40) and (41). In addition, we take Π_2 as the Poincaré section and obtain Figure 4(d) by direct numerical simulation. As shown in Figures 4(c) and 4(d), there exists the local attractor near grazing bifurcation.

Fixed parameters $\mu_m = 6.0$, $\mu_k = 3.0$, $\omega = 0.5649677$, $R = 0.82$, $\zeta = 0.2$, $p = 0.813$. the critical value$d^* = 1.821554$, such that $h_x^{D_1}(x^{*1})(N_2 N_1)^5 \beta_1 = 0$. It corresponds to the codimension-two grazing bifurcation. We obtain the bifurcation diagram Figure 2(e) through numerical simulation by the discontinuity maps (19) and (20). As shown in Figure 2(e), the system is in a complex chaotic state near the grazing point. Then, we take Π_2 as the Poincaré section and obtain Figure 2(f) by direct numerical simulation.

Based on the control strategy mentioned in Section 4, we select $k_1 = -0.6$, $k_3 = -1$, $k_4 = -0.6$, and $k_6 = -1$ as the fixed parameters; a two-dimensional control region graph of k_2 and k_5 is obtained as shown in Figure 3(c), where k_2 is $x-$axis, k_5 is $y-$axis, and the blue region is the region of control parameters for suppressing the chaos. Then, we select $k_2 = -5.8$ and $k_5 = -5.8$ to control the system, and the bifurcation diagram is obtained as shown in Figure 4(e) by the discontinuity maps (40) and (41). In addition, we take Π_2 as the Poincaré section and obtain Figure 4(f) by direct numerical simulation.

Comparing Figure 2 with Figure 4, it is shown that the results obtained by mappings are in good agreement with the direct numerical simulation, and the control effect is further verified.

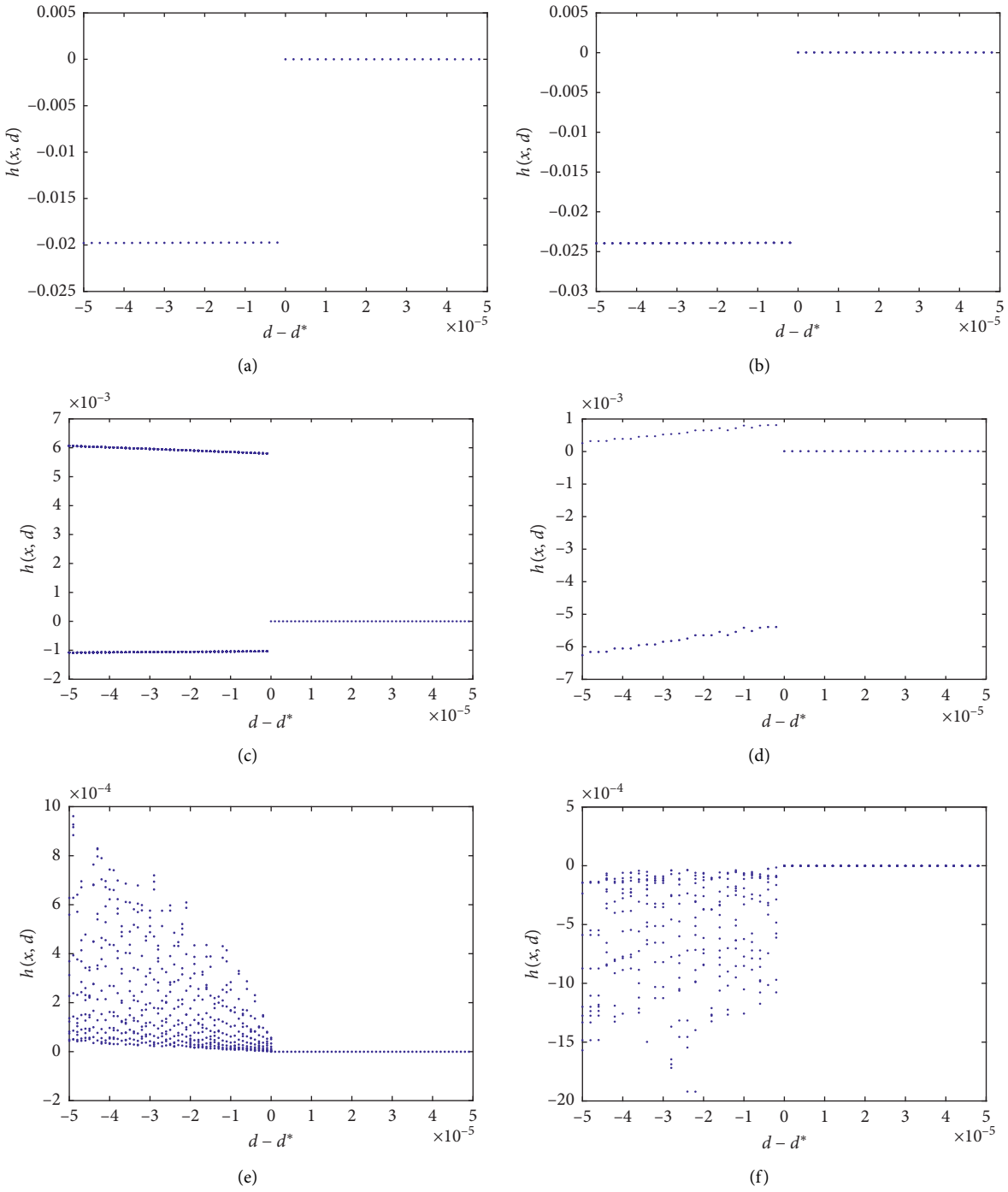

Figure 2: Bifurcation diagram from the grazing bifurcation. (a) (1/1) impact periodic motions based on the numerical simulation obtained by the discontinuity maps (19) and (20). (b) Direct numerical simulation on Poincaré section Π_2 of (1/1) impact periodic motions. (c) (1/2) impact periodic motions based on the numerical simulation obtained by the discontinuity maps (19) and (20). (d) Direct numerical simulation on Poincaré section Π_2 of (1/2) impact periodic motions. (e) The codimension-two grazing bifurcation points based on the numerical simulation obtained by the discontinuity maps (19) and (20). (f) Direct numerical simulation on Poincaré section Π_2 of the codimension-two grazing bifurcation points.

6. Conclusions

The discontinuous grazing bifurcation is often accompanied by a jump phenomenon. In addition, complex chaotic regions occur near the codimension-two bifurcation points. How to avoid the dramatic change of system response caused by jump phenomenon of grazing bifurcation or the codimension-two bifurcation point is an urgent requirement for the control mechanism of discontinuous grazing bifurcation. In this paper, a discrete-in-time feedback control

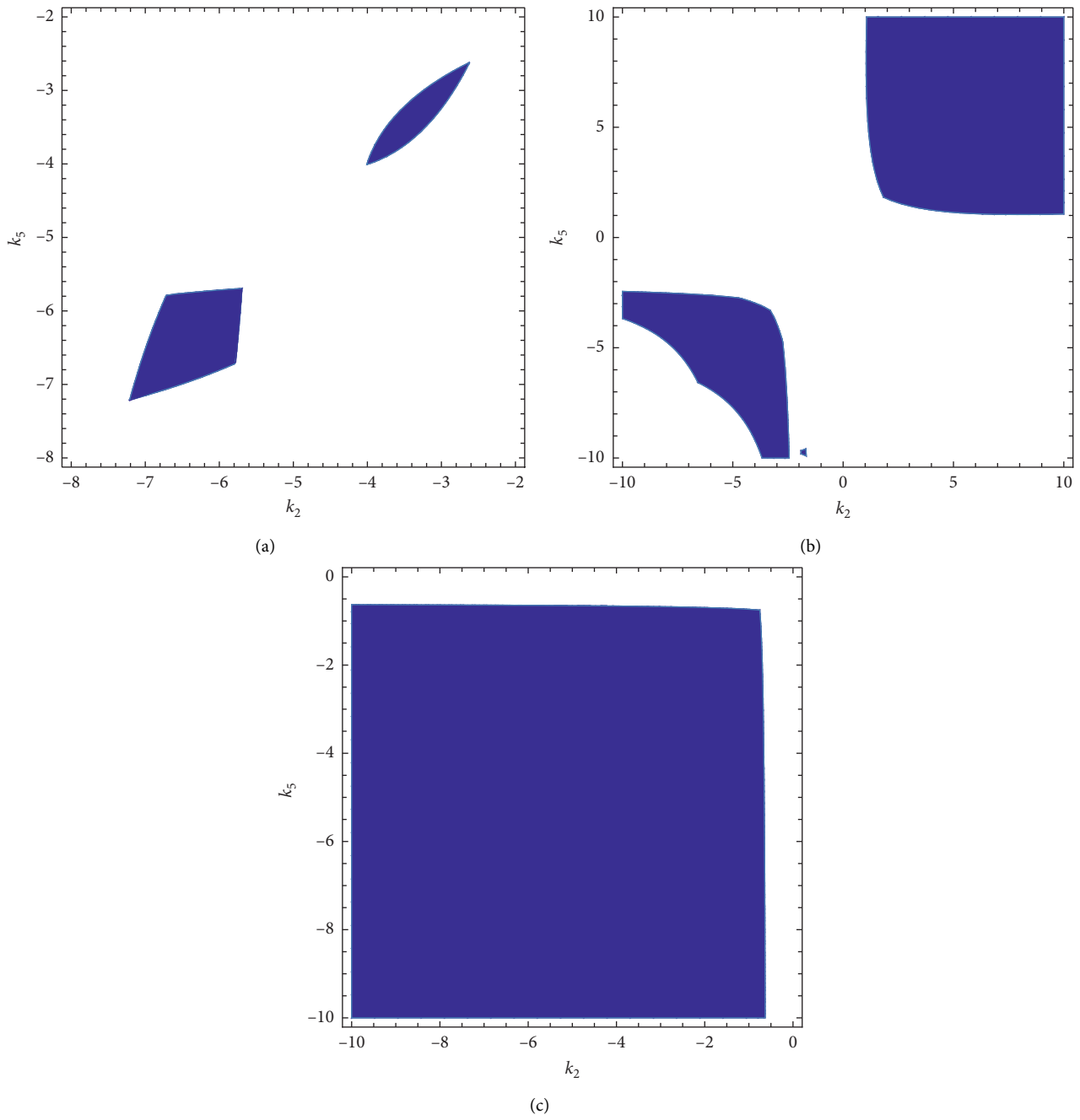

FIGURE 3: The parameters k_2 and k_5 control region. (a) The grazing bifurcation of (1/1) impact periodic motions. (b) The grazing bifurcation of (1/2) impact periodic motions. (c) The codimension-two grazing bifurcation points.

strategy is used to control the near-grazing dynamics of double grazing period motion in a two-degree-of-freedom vibroimpact system with symmetrical constraints. Compared to unilateral constrained systems, the stability criterion of double grazing period motion becomes more complex. Based on the stability criterion, the control strategy is designed to control the near-grazing dynamics and the two parameters' control region is obtained. For the case of discontinuous grazing bifurcation, we take two jumping phenomena (jumping from nonimpact periodic motion to (1/1) and (1/2) impact periodic motion) as examples to stabilize grazing bifurcation by controlling the parameters

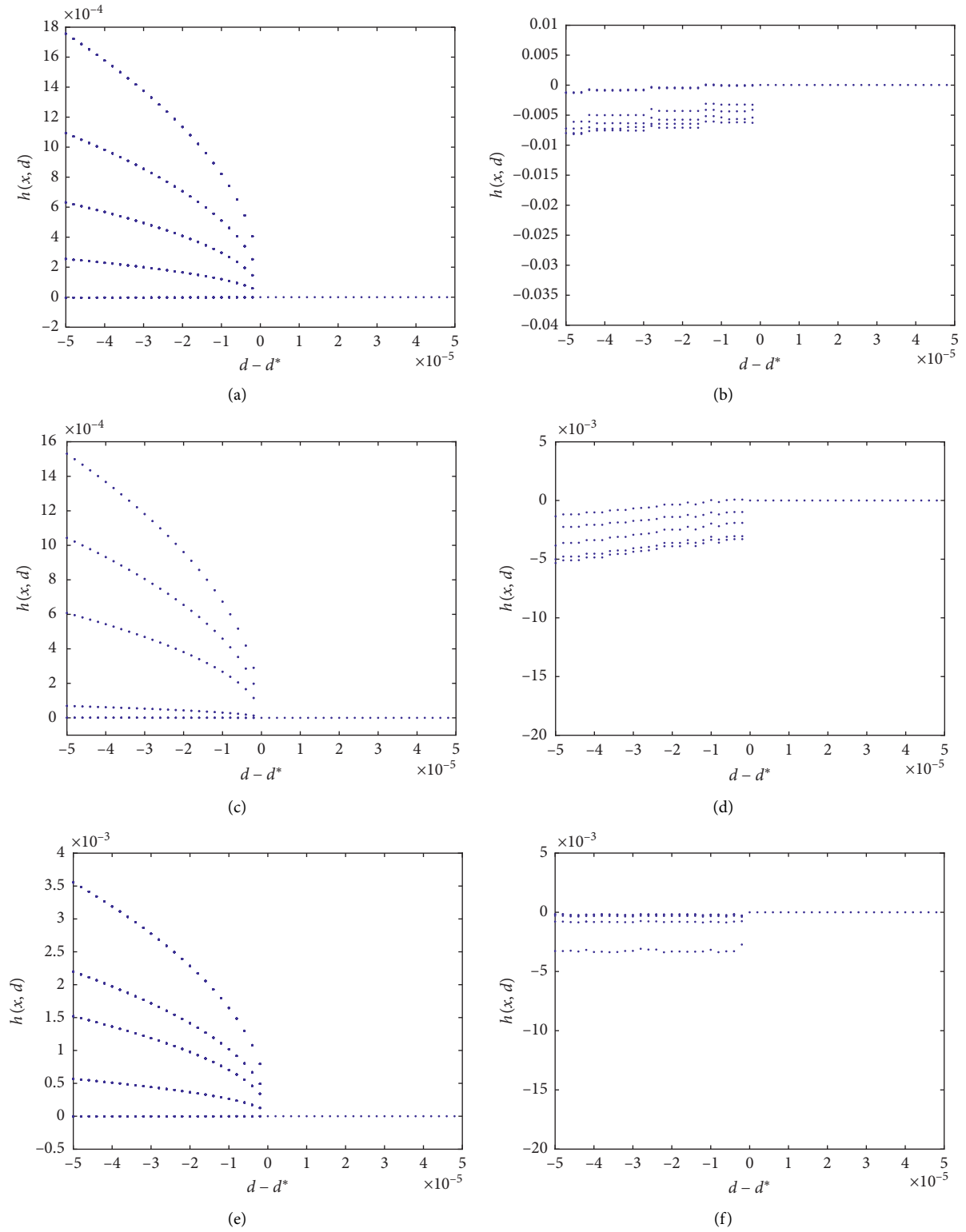

Figure 4: Bifurcation diagram of a stable grazing bifurcation after control. (a) (1/1) impact periodic motions based on the numerical simulation obtained by the discontinuity maps (38) and (39). (b) Direct numerical simulation on Poincaré section Π_2 of (1/1) impact periodic motions. (c) (1/2) impact periodic motions based on the numerical simulation obtained by the discontinuity maps (38) and (39). (d) Direct numerical simulation on Poincaré section Π_2 of (1/2) impact periodic motions. (e) The codimension-two grazing bifurcation points based on the numerical simulation obtained by the discontinuity maps (38) and (39). (f) Direct numerical simulation on Poincaré section Π_2 of the codimension-two grazing bifurcation points.

on the controller. In addition, the chaos dynamics near codimension-two grazing bifurcation point is controlled by using this strategy. Finally, the feasibility of the control strategy is illustrated by comparing the numerical simulation of composite mapping with the direct numerical simulation of Poincare section.

Data Availability

The simulation data used to support the findings of this study are included within the article.

Conflicts of Interest

The authors declare that they have no conflicts of interest.

Acknowledgments

This study was supported by the project sponsored by the National Natural Science Foundation of China (nos. 11602059 and 11872154) and Guangxi Natural Science Foundation (no. 2018JJA110046).

References

[1] A. B. Nordmark, "Non-periodic motion caused by grazing incidence in an impact oscillator," *Journal of Sound and Vibration*, vol. 145, no. 2, pp. 279–297, 1991.

[2] A. B. Nordmark, "Universal limit mapping in grazing bifurcations," *Physical Review E*, vol. 55, no. 1, pp. 266–270, 1997.

[3] M. Bernardo, C. Budd, A. R. Champneys et al., *Piecewise-smooth Dynamical Systems: Theory and Applications*, Springer Science and Business Media, Berlin, Germany, 2008.

[4] H. Dankowicz and M. Katzenbach, "Discontinuity-induced bifurcations in models of mechanical contact, capillary adhesion, and cell division: a common framework," *Physica D: Nonlinear Phenomena*, vol. 241, no. 22, pp. 1869–1881, 2012.

[5] G. Wen, H. Xu, L. Xiao, X. Xie, Z. Chen, and X. Wu, "Experimental investigation of a two-degree-of-freedom vibro-impact system," *International Journal of Bifurcation and Chaos*, vol. 22, Article ID 1250110, 2012.

[6] S. Banerjee, J. Ing, E. Pavlovskaia, M. Wiercigroch, and R. K. Reddy, "Invisible grazings and dangerous bifurcations in impacting systems: the problem of narrow-band chaos," *Physical Review E*, vol. 79, Article ID 037201, 2009.

[7] D. R. J. Chillingworth, "Dynamics of an impact oscillator near a degenerate graze," *Nonlinearity*, vol. 23, no. 11, pp. 2723–2748, 2010.

[8] N. Humphries and P. T. Piiroinen, "A discontinuity-geometry view of the relationship between saddle-node and grazing bifurcations," *Physica D: Nonlinear Phenomena*, vol. 241, no. 22, pp. 1911–1918, 2012.

[9] M. H. Fredriksson and A. B. Nordmark, "Bifurcations caused by grazing incidence in many degrees of freedom impact oscillators," *Proceedings of the Royal Society of London. Series A: Mathematical, Physical and Engineering Sciences*, vol. 453, no. 1961, pp. 1261–1276, 1997.

[10] P. Thota and H. Dankowicz, "Continuous and discontinuous grazing bifurcations in impacting oscillators," *Physica D: Nonlinear Phenomena*, vol. 214, no. 2, pp. 187–197, 2006.

[11] P. Kowalczyk, M. di Bernardo, A. R. Champneys et al., "Two-parameter discontinuity-induced bifurcations of limit cycles: classification and open problems," *International Journal of Bifurcation and Chaos*, vol. 16, no. 03, pp. 601–629, 2006.

[12] S. Foale, "Analytical determination of bifurcations in an impact oscillator," *Philosophical Transactions of the Royal Society of London. Series A: Physical and Engineering Sciences*, vol. 347, no. 1683, pp. 353–364, 1994.

[13] P. Thota, X. Zhao, and H. Dankowicz, "Co-dimension-two grazing bifurcations in single-degree-of-freedom impact oscillators," *Journal of Computational and Nonlinear Dynamics*, vol. 1, no. 4, pp. 328–335, 2006.

[14] J. Xu, P. Chen, and Q. Li, "Theoretical analysis of co-dimension-two grazing bifurcations in *n*-degree-of-freedom impact oscillator with symmetrical constrains," *Nonlinear Dynamics*, vol. 82, no. 4, pp. 1641–1657, 2015.

[15] A. Colombo and F. Dercole, "Discontinuity induced bifurcations of nonhyperbolic cycles in nonsmooth systems," *SIAM Journal on Applied Dynamical Systems*, vol. 9, no. 1, pp. 62–83, 2010.

[16] H. Jiang, A. S. E. Chong, Y. Ueda, and M. Wiercigroch, "Grazing-induced bifurcations in impact oscillators with elastic and rigid constraints," *International Journal of Mechanical Sciences*, vol. 127, pp. 204–214, 2017.

[17] S. Yin, Y. Shen, G. Wen, and H. Xu, "Analytical determination for degenerate grazing bifurcation points in the single-degree-of-freedom impact oscillator," *Nonlinear Dynamics*, vol. 90, no. 1, pp. 443–456, 2017.

[18] H. Dankowicz and X. Zhao, "Local analysis of co-dimension-one and co-dimension-two grazing bifurcations in impact microactuators," *Physica D: Nonlinear Phenomena*, vol. 202, no. 3-4, pp. 238–257, 2005.

[19] X. Zhao and H. Dankowicz, "Unfolding degenerate grazing dynamics in impact actuators," *Nonlinearity*, vol. 19, no. 2, pp. 399–418, 2005.

[20] H. Dankowicz and J. Jerrelind, "Control of near-grazing dynamics in impact oscillators," *Proceedings of the Royal Society A: Mathematical, Physical and Engineering Sciences*, vol. 461, no. 2063, pp. 3365–3380, 2005.

[21] H. Dankowicz and F. Svahn, "On the stabilizability of near-grazing dynamics in impact oscillators," *International Journal of Robust and Nonlinear Control*, vol. 17, no. 15, pp. 1405–1429, 2007.

[22] S. Misra and H. Dankowicz, "Control of near-grazing dynamics and discontinuity-induced bifurcations in piecewise-smooth dynamical systems," *International Journal of Robust and Nonlinear Control*, vol. 20, pp. 1836–1851, 2010.

[23] S. Yin, G. Wen, and X. Wu, "Suppression of grazing-induced instability in single degree-of-freedom impact oscillators," *Applied Mathematics and Mechanics*, vol. 40, no. 1, pp. 97–110, 2019.

[24] H. Xu, S. Yin, G. Wen, S. Zhang, and Z. Lv, "Discrete-in-time feedback control of near-grazing dynamics in the two-degree-of-freedom vibro-impact system with a clearance," *Nonlinear Dynamics*, vol. 87, no. 2, pp. 1127–1137, 2017.